J. Appl. Comput. Mech., 5(4) (2019) 680-695
DOI: 10.22055/JACM.2019.27402.1399

ISSN: 2383-4536
jacm.scu.ac.ir

M&MoCS

Shahid Chamran University of Ahvaz

Journal of Applied and Computational Mechanics

Research Paper

Introduction to the Slide Modeling Method for the Efficient Solution of Heat Conduction Calculations

Mehran Vagheian[1], Saeed Talebi[2]

[1] Department of Energy Engineering and Physics, Amirkabir University of Technology (Tehran Polytechnic)
424 Hafez Avenue, P.O. Box 15875-4413, Tehran, Iran, Email: mvagheian@aut.ac.ir

[2] Department of Energy Engineering and Physics, Amirkabir University of Technology (Tehran Polytechnic)
424 Hafez Avenue, P.O. Box 15875-4413, Tehran, Iran, Email: sa.talebi@aut.ac.ir

Received October 23 2018; Revised December 19 2018; Accepted for publication January 12 2019.
Corresponding author: Mehran Vagheian, mvagheian@aut.ac.ir

Abstract. Determination of the maximum temperature and its location is the matter of the greatest importance in many technological and scientific engineering applications. In terms of numerical calculations of the heat conduction equation by using uniform mesh increments in space, large computational cost is sometimes countered. However, adaptive grid refinement method could be computationally efficient both in terms of accuracy and execution time. In this work, the numerical solution of the heat conduction equation based on the slide modeling method (SMM) is introduced. This method is based on a pre-determined mesh density approach which divides each homogeneous region into different slides and then assigns higher mesh point densities to slides of interest regarding their relative importance by performing some mathematical calculations. The importance of each region is determined by some formulated weighting factors which rely on the estimation of temperature profiles in all regions and slides. To investigate the accuracy and efficiency of the proposed method, a number of different case studies have been considered. The results all revealed the strength of the proposed SMM in comparison with the conventional method (based on uniform mesh point distribution).

Keywords: Slide modeling method, Efficient finite volume method, Heat conduction calculations, Unstructured meshes.

1. Introduction

Determination of the maximum temperature and its location is the matter of the greatest importance in many technological and scientific engineering applications. This is mainly due to the fact that in a homogeneous region, required information, including the exact temperatures as well as the location of the maximum temperature are always essential to prevent local abnormal conditions [1, 2]. In consequence, there is a strong incentive to develop accurate and computationally efficient methods for obtaining these parameters.

A number of methods have been developed and introduced for solving the heat conduction equation such as the Finite Difference Method (FDM) [3], Finite Element Method (FEM) [4], Finite Volume Method (FVM) [5], Discrete Element Method (DEM) [6], Boundary Element Method (BEM) [7], Monte Carlo Method (MCM) [8] and Meshless Method [9]. Among the aforementioned methods, the FDM has been always the center of attention on account of its simplicity and satisfactory accuracy [10, 11].

Previous research findings suggests that the discretization forms of differential equations by the FDM can mainly be divided into two categories, namely Mesh-Edged and Mesh-Centered. It is also worth to mention that the latter, which is also called as the Box-Scheme FDM gives almost a more accurate numerical solution in comparison to the other one [11].

As is obvious, the accuracy of the FDM can significantly be impacted by changing the number of mesh elements. However,

Published online: May 01 2019

it is also revealed that the position of mesh elements is a second key factor that should be considered. In fact, there are numbers of mesh adaptive approaches for optimizing mesh point positions and consequently, the selection and development of an innovative approach are the center of attention that has been discussed widely in the literature for different numerical problems [11-18].

Based on the arguments mentioned above, it is evident that distributing the mesh point positions is almost the center of attention, and accordingly a number of different perspectives have been applied for different applications. In 2015, Zhai et al. [14] has shown that an adaptive local mesh refinement could be considered with respect to the unknown variable errors along with its first derivatives where a higher mesh element density is applied in domain with rapid function variations in comparison to the other regions with relatively smooth variations. Recently, Zhai et al. [15] have also presented an improved scheme for the convection-dominated diffusion solution by using a non-uniform grid structure method. This work has also supported the fact that the accuracy of the non-uniform grids is significantly higher than those using uniform grids. Cao et al. [12] investigated a hybrid adaptive Finite Difference Method to form an unstructured-based mesh method by using the posteriori error estimation technique. Based on the suggested method, three principal numerical steps are considered, including: a finite difference solver, a posteriori error estimator, and a re-gridding re-coarsening tool. Here, the error estimation is determined by solving a local Neumann problem to form an error energy norm for guiding the mesh adaptation through the simultaneous mesh refinement process. It has been shown that by implementing this method, the global error magnitude has been eventually reduced. In addition to the error estimation approach, some researchers have introduced different types of view of methodology for optimization problems. In this connection, Lee et al. [13] developed a novel technique based on the finite difference moving mesh method to provide higher accuracy of the one-dimensional nonlinear initial value problems. According to this adaptive method, the mesh point distribution is adjusted to focus on areas of interest where the solution of the problem varies with rapid changes. The results showed that the accuracy of the solution has been significantly developed. The finite difference weighted essentially non-oscillatory method (WENO) may alternatively be used to refine mesh distributions [3]. Regard to this approach, it has been shown that the accuracy of the solution along with the performance of the numerical calculation can be remarkably improved by getting the way for using a new cell-based data structure to form the adaptive meshes of multi-dimensional denotation problems.

In 2016, a pre-determined mesh point position technique was developed to increase the efficiency and accuracy of the nuclear reactor calculations using an adaptive BSFDM [11]. This method considered the two key mentioned parameters concomitantly, i.e. the number of mesh elements and the adaptively mesh refinement. According to the proposed method, the mesh positions are pre-determined in all regions by considering each region's importance in the solution. In facilitating consistent accuracy comparison, the results of the proposed adaptive method and the standard FDM is presented for the same number of mesh elements. This method proved its strength on obtaining more accurate results for any arbitrary the same number of mesh elements.

Our application of interest is the determination of the maximum temperature and its corresponding locations using the heat conduction calculations based on the SMM. This proposed method is based on dividing each homogeneous region into different slides and then calculating the relative importance of them using the formulated weighting factors which rely on the estimation of temperature profiles in all slides. The formalism for derivation of the mathematical conduction equation is performed using the BSFDM (Box-Scheme Finite Difference Method) and solved numerically by the iteration method. To consider the strength of the proposed method properly, it accounts for different type of boundary conditions and mesh point numbers. For a quantitative comparison, the total involved CPU time is reported for the same level of accuracy between the proposed SMM method and the CM (based on uniform mesh distribution).

The current research is organized in six sections. In the second section, the adaptive discretization form of the governing equations for one and two-dimensional rectangular geometries are presented. These equations are derived based on the BSFDM used for iterative calculating. In section three, the proposed SMM method is completely introduced and followed by the required mathematical equations and methodology. In the fourth section, the proposed method is applied to five different problems, including the two aforementioned rectangular geometries to verify and evaluate the results of the calculations for different boundary conditions and temperature distributions. For facilitating comparison purpose, the total CPU time of the calculations has also been presented in this section to study the efficiency of the suggested SMM method. In the section five, the discussion of the obtained results has been presented and finally, in the last section a conclusion of the paper has been stated.

2. Mathematical Formulation

In this section, the numerical solution scheme for the temperature distributions with one and two-dimensional heat conduction equations are presented. This section, deals primarily with one-dimensional steady-state cases in which the discretization adaptive form of the governed equations based on the BSFDM is introduced. Following this, the process is repeated, beginning by illustrating the derivation of the governed equations for two-dimensional rectangular geometries by considering non-equal mesh box sides.

2.1. Adaptive one-dimensional heat conduction approach

In this subsection, the heat transfer by conducting in one-dimensional geometry is stressed. The general form of the mentioned equation is as the following [19, 20]:

$$U\frac{\partial^2 T}{\partial x^2}=-q''', \tag{1}$$

This equation is the stationary form of the heat transfer by conducting in one-dimensional geometry and known as Poisson's equation. In eq. (1), q''' is the volumetric thermal source strength and U is the heat conduction coefficient. The volumetric thermal source is applied in the heat transfer equation due to the consideration of possible existence of internal heat generation in the material. Hence, for the development of the proposed method in this work, a general heat conduction equation, which can be used to evaluate the heat transfer in any direction and with or without heat generation, is considered. In the following, the discretization procedure of the aforementioned equation is presented in details.

As can be observed from Fig.1, the implementation can be carried out by considering the two adjacent neighbors for *i*th mesh box, in such a way that in the resulting mesh, nodal points fell on in the center of a mesh box based on the BSFDM. It is noticeable that, Δ^i and Δ^j reflecting the side length of *i*th mesh box and the adjacent neighbors $j=[1,2]$, respectively.

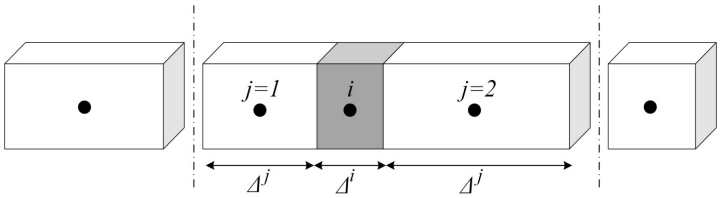

Fig. 1. Two adjacent neighbors of box (*i*) in 1-D geometry

The discretized scheme of the one dimensional heat conduction equations can be widely found in the literature; however, we propose a reformulation of these equations using non-equal mesh box approach as follows:

$$\sum_{j=1}^{2}\oint_s q''ds=\int_V q'''dV, \tag{2}$$

where all parameters have their usual meaning. In order to obtain q'' in eq. (2), one can employ eq. (3) and obtain eqs. (4) and (5):

$$q''=-U\frac{dT}{dx}, \tag{3}$$

$$q''_{in}=-U^j\frac{T^j-T_s}{\Delta^j/2}, \tag{4}$$

$$q''_{out}=-U^i\frac{T_s-T^i}{\Delta^i/2}, \tag{5}$$

In eqs. (4) and (5), T_s is the temperature at shared interface between box (*i*) and box (*j*). Because, this parameter is not determined using the cell centered FVM, it should be substituted with another parameter. This can be performed regarding the fact that in the shared interface $q''_{in}=q''_{out}$, accordingly, one can obtain:

$$T_s=\frac{\left(U^i/\Delta^i\right)T^i+\left(U^j/\Delta_j\right)T_j}{\left(U_i/\Delta_i+U_j/\Delta_j\right)}. \tag{6}$$

By substituting T_s from eq. (6) into eqs. (4) and (5) and then considering q''_{net}, one has:

$$q''_{net}=\frac{-2U^j\times U^i}{U^j\times\Delta^i+U^i\times\Delta^j}\left(T_j-T_i\right), \tag{7}$$

Finally, by substituting eq. (7) into eq. (2) one can obtain the discretized form of the heat transfer equation on 1-D geometries and for box (*i*) as:

$$\sum_{j=1}^{2}\left[2\frac{U^i\times U^j}{U^i\times\Delta^j+U^j\times\Delta^i}\right]\times T^i+\sum_{j=1}^{2}\left[-2\frac{U^i\times U^j}{U^i\times\Delta^j+U^j\times\Delta^i}\right]\times T^j=q'''\times\Delta^i, \tag{8}$$

In eq. (8), all parameters have their usual meaning. It is noteworthy to mention that we want to apply our presented algorithm for 1 and 2 dimensional geometries considering different boundary conditions. More precisely, the capability of the proposed method has been the center of our attention to prove the effectiveness and efficiency of the method in different conditions. Regarding eq. (8), it is obvious and vivid that this equation is a general form of the 1-D heat conduction equation with two adjacent neighbors; however, it is rewarding to demonstrate the governed equations with respect to different boundary conditions for boundary CVs [1, 2]. In the first case, the mesh box (i), is subjected to a constant and uniform wall temperature. So, one can rewrite eq. (7) for the boundary face as:

$$q''_{net} = -\frac{U^i}{\Delta^i/2}\left(T_s - T^i\right), \tag{9}$$

So, the governing heat conduction equation for the boundary CV can be simply derived as the following:

$$\left[\sum_{j=1}^{2} 2\frac{U^i \times U^j}{U^i \times \Delta^j + U^j \times \Delta^i} + 2\frac{U^i}{\Delta^i}\right] \times T^i + \left[\sum_{j=1}^{2} -2\frac{U^i \times U^j}{U^i \times \Delta^j + U^j \times \Delta^i}\right] \times T^j + \left[-2\frac{U^i}{\Delta^i}\right] \times T_s = q''' \times \Delta^i. \tag{10}$$

In the same way, in the case of the insulation boundary condition [1, 2] one can have for the boundary face:

$$q''_{net} = 0, \tag{11}$$

and subsequently one can express the discretized heat conduction equation for the boundary CV for node (i) as follows:

$$\left[\sum_{j=1}^{2} 2\frac{U^i \times U^j}{U^i \times \Delta^j + U^j \times \Delta^i}\right] \times T^i + \left[\sum_{j=1}^{2} -2\frac{U^i \times U^j}{U^i \times \Delta^j + U^j \times \Delta^i}\right] \times T^j = q''' \times \Delta^i. \tag{12}$$

We can now analyze problems in which a wall cooled by flowing fluid on one side of the boundary mesh box (i). By considering this boundary condition, one can obtain for the boundary face:

$$\frac{-U^i}{\Delta^i/2}(T_s - T^i) = h(T_s - T_f), \tag{13}$$

By rearranging eq. (13), one can obtain:

$$T_s = \frac{\left(2U^i/\Delta \times h\right)T^i + T_f}{1 + \left(2U^i/\Delta \times h\right)}, \tag{14}$$

And then, rewrite the governing equation for the boundary CV (i) as:

$$\left[\sum_{j=1}^{2} \frac{2 \times U^i \times U^j}{U^i \times \Delta^j + U^j \times \Delta^i} + \frac{2 \times U^i \times h}{\Delta^i \times h + 2 \times U^i}\right] \times T^i + \sum_{j=1}^{2}\left[-\frac{2 \times U^i \times U^j}{U^i \times \Delta^j + U^j \times \Delta^i}\right] \times T^j + \left[\left(-\frac{2 \times U^i \times h}{\Delta^i \times h + 2 \times U^i}\right) \times T_f\right] = q''' \times \Delta^i, \tag{15}$$

Where h and T_f are the heat transfer coefficient and temperature of the flow, respectively. In addition to the discussed boundary conditions, one can also consider the mixed boundary conditions such as thermal radiation and heat convection. According to the procedure of discretization which has been presented previously in this work, the main step is obtaining the temperature of boundary face (i.e. T_s) and then using it to obtain the discretized governing equation. On this basis, a boundary face that has thermal radiation and heat convection boundary conditions is considered regarding the assumption that these boundary conditions are separated and do not have any impact on each other. Accordingly, one can have:

$$-U^i \frac{T_s - T_i}{\Delta/2} = h(T_s - T_f) - \alpha\sigma T_f^4, \tag{16}$$

where all parameters have their usual meaning. By rearranging eq. (16), one can obtain:

$$T_s = \left(\frac{\left(2U^i/\Delta\right)}{h + \left(2U^i/\Delta\right)}\right)T^i + \frac{h}{h + \left(2U^i/\Delta\right)}T_f + \frac{\alpha\sigma}{h + \left(2U^i/\Delta\right)}T_f^4, \tag{17}$$

Using eq. (17) one can obtain the governing heat equation similar to the previous cases. Due to the fact that there are more mixed boundary conditions that can be also considered, we did not investigate further these kind of problems.

At this stage it is instructive to evaluate the temperature distributions using the BSFDM approximation. To solve the

discretized governing equations numerically, the mentioned parameters can be searched for an iterative process. This method consists of successive steps, where, at first estimating initial values typically proceed for the unknown temperatures at all nodal points and subsequently the temperatures are recalculated using the new adjacent and previous adjoining temperatures. This iterative process is continued until some convergence criteria regarding the temperatures all are fulfilled [10, 11, 19, and 20].

2.2. Adaptive two-dimensional heat conduction approach

In this section, introducing the discretization form of the two-dimensional heat conduction equations based on the BSFDM is presented. The general 2-D heat conduction equation is considered as follows [1, 2]:

$$U\frac{\partial^2 T}{\partial x^2}+U\frac{\partial^2 T}{\partial y^2}=-q''', \tag{18}$$

As can be seen, eq. (18) is the general form of the heat conduction equations and consequently it should be discretized similar to the case of 1-D geometry. Fig. 2 illustrates the 2-D structured rectangular geometry by considering the four adjacent neighbors.

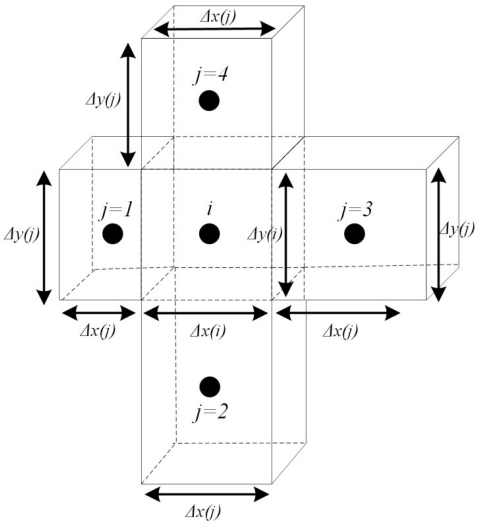

Fig. 2. Four adjacent neighbors of box (*i*) in 2-D geometry

As can be seen, each side of a mesh box is assumed to be differed from the surrounding boxes regarding the adaptive approach. From this figure, it is also clear that Δx and Δy imply the side lengths of a mesh box in x and y direction, respectively. For discretization of the governing heat conduction equation in 2-D geometries, one has:

$$\sum_{j=1}^{4}\oint_s q''ds=\int_V q'''dV, \tag{19}$$

Using eq. (19), the discretized form of the adaptive governing equation in the case of 2-D geometries can be obtained similar to the 1-D geometries as:

$$\sum_{j=1}^{4}\left[2\frac{U^i\times U^j}{U^i\times\Delta^j+U^j\times\Delta^i}\times S^i\right]\times T^i+\sum_{j=1}^{4}\left[-2\frac{U^i\times U^j}{U^i\times\Delta^j+U^j\times\Delta^i}\times A^i\right]\times T^j=q'''\times V^i, \tag{20}$$

Here, S^i and V^i are the area and volume of ith mesh box, respectively. It is also noteworthy to mention that, in eq. (20) Δ is as Δx or Δy depending on which direction is chosen. Moreover, as is shown in Fig. 2, one can reasonably argue that A is perpendicular to the side of Δ. In order to obtain the governing discretized equation of the boundary CVs, each face of the CV should be treated separately similar to the 1-D geometries. In the following, discretization of one corner CV in a 2-D geometry is considered.

As is observable in Fig. (3), the right boundary face is exposed to a heat flux (q''_{Right}) and the bottom boundary condition is reflective (i.e. $\partial T/\partial y=0$ on the boundary). So, one can simply consider:

$$\oint_{S_{Right}} q''_{Right}ds+\oint_{S_{Left}} q''_{Left}ds+\oint_{S_{Top}} q''_{Top}ds+\oint_{S_{Bottom}} q''_{Bottom}ds=\int_V q'''dV. \tag{21}$$

In the case of the corner CV, by considering the right and bottom boundary conditions, one can have:

$$\oint_{S_{Right}} q''_{Right}ds=q''_{Right}\times\Delta y^i, \tag{22}$$

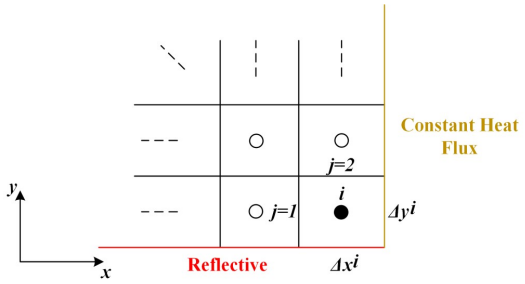

Fig. 3. Schematic view of the corner CV in 2-D geometries

$$\oint_{S_{Bottom}} q''_{Bottom} ds = 0. \tag{23}$$

In the case of the left and top boundary faces, previously the equations were derived (for 1-D geometries), So:

$$\oint_{S_{Left}} q''_{Left} ds = \frac{-2U^1 \times U^i}{U^1 \times \Delta x^i + U^i \times \Delta x^1} \times \Delta y^i \times (T_1 - T_i), \tag{24}$$

$$\oint_{S_{Top}} q''_{Top} ds = \frac{-2U^2 \times U^i}{U^2 \times \Delta y^i + U^i \times \Delta y^2} \times \Delta x^i \times (T_2 - T_i). \tag{25}$$

Thus, one can simple consider the discretized governing equation for the boundary corner CV as:

$$\begin{aligned} &\left\{\frac{-2U^1 \times U^i}{U^1 \times \Delta x^i + U^i \times \Delta x^1} \times \Delta y^i\right\} \times T_1 + \left\{\frac{-2U^2 \times U^i}{U^2 \times \Delta y^i + U^i \times \Delta y^2} \times \Delta x^i\right\} \times T_2 \\ &+ \left\{\left(\frac{+2U^1 \times U^i}{U^1 \times \Delta x^i + U^i \times \Delta x^1} \times \Delta y^i\right) + \left(\frac{+2U^2 \times U^i}{U^2 \times \Delta y^i + U^i \times \Delta y^2} \times \Delta x^i\right)\right\} \times T_i \\ &+ \left\{q''_{Right} \times \Delta y^i\right\} = q''' \times \Delta x^i \times \Delta y^i. \end{aligned} \tag{26}$$

To solve eq. (26), it is convenient to employ the numerical techniques including the iterative process which are formally mentioned in the previous section for one-dimensional calculations. It should be noted that the above equation is the general form of the 2-D heat conduction equation and consequently by considering the different boundary conditions, the corresponding formulas can simply be derived similar to the 1-D approach.

3. The Proposed SMM

The aim of this section is to introduce the SMM with application in the heat conduction calculations for both one and two-dimensional rectangular geometries. It is widely shown in the literature that in most engineering and industrial heat transfer problems such as irradiated slab media, nuclear plate-type fuel elements, cladding plate-type fuel elements, electrical equipment, mechanical equipment, and other uncomplicated structures which the temperature distribution is not varied dramatically, the temperature distribution mainly follows a quadratic curve in the presence of a space-independent volumetric heat source (it also depends on boundary conditions) [1, 2, 19 and 20]. Considering this point and the fact that, at least three points are always required to estimate a quadratic curve; each homogeneous region can be divided into three different slides and then a coarse heat conduction calculation can be implemented to determine the approximated distribution of the temperature profile in the regions and the corresponding slides. Using the results of these preliminary mathematical calculations, one can assign higher mesh point densities to slides of interest regarding their relative importance in each region. The importance of each slide can be determined by some formulated weighting factors which rely on the estimation of temperature profiles in all slides. On this basis, the maximum temperatures and their corresponding locations in different regions with different material properties can be determined by considering a higher spatial resolution. This method of implementation can provide high computational efficiency in addition to the global high accuracy. It is also worth pointing out that, another key feature which has been taken into account is the capability of using any arbitrary mesh point numbers in designing the proposed method. Needless to say that, this factor is essentially needed for evaluating the obtained results against the usual methods with the same number of nodal mesh points [11].

To explain the procedure of the developed method properly, this section has been divided into two parts. The first part deals with the one-dimensional approach, and the second part provides the adaptive mathematical formulation considering the two-dimensional geometry.

3.1. One-dimensional SMM

Using the points mentioned above and considering the 1-D approach, the proposed adaptive method can be presented via the stepwise algorithm described below:

1) Divide the entire geometry of a homogeneous structure into three slides as eq. (27):

$$\text{Silde Dimension} = \frac{A}{3}, \tag{27}$$

where A refers to the dimension of region and Slide Dimension indicates the dimension of each slide in the region. Then, calculating the heat conduction equations to approximate the temperature profile is performed. It should be underlined that if a multi-structure with different materials is desired, each structure should be treated separately to form the mentioned slides in each homogeneous region as eq. (28).

$$\text{Silde Dimension}_{\text{m}} = \frac{A}{3}, \quad m = 1,2,...,M \tag{28}$$

where m refers to the number of each homogeneous region in the problem.

2) Calculate a set of weighting factors to assign a fraction of the appropriate number of mesh points for each slide. These weighting factors are determined with respect to the obtained temperature values from the previous step as the following:

$$SWF_g = \sum_{g=1}^{3} T^g, \quad g = 1,\ 2 \text{ and } 3 \tag{29}$$

where g is the slide number in each region and SWF_g refers to the Slide Weighting Factor g. Due to the fact that the weighting factor is a summation of a number of temperatures, accordingly, it has the dimension of Celsius degrees. By implementing this step, one can determine the importance of each slide in each region. In the case of multi-regions, there are three SWF for each region. Accordingly, one can rewrite eq. (29) as:

$$SWF_{m,g} = \sum_{g=1}^{3} T^{m,g}, \quad g = 1,\ 2 \text{ and } 3 \tag{30}$$

where $SWF_{m,g}$ and $T^{m,g}$ are the Slide Weighting Factor of slide g in region m and temperature of slide g in region m. To assign different mesh resolutions in each slide with an arbitrary total mesh point number (determined by users), implantation of the next step is needed.

3) Determine the appropriate number of meshes corresponding to each slide as follows:

$$\frac{SWF_g}{\sum_g SWF_g} \times W = d_g, \tag{31}$$

where d_g is the mesh point numbers in the corresponding slide g, and W implies the total number of mesh elements. It is worth bearing in mind that, as is also mentioned before, the SWF_g needs to be calculated for each slide in a homogeneous region. In other words, in the case of a multi-region case, the weighting factors should be evaluated separately regarding the maximum temperature in each region. This allows to properly extract this parameter as accurate as possible in the respective regions. In fact, in the case of multi-region, one can rewrite eq. (31) as:

$$\frac{SWF_{m,g}}{\sum_g SWF_{m,g}} \times W_m = d_{m,g}, \tag{32}$$

here $d_{m,g}$ is the mesh point numbers in slide g and region m, and, W_{m} implies the total number of mesh elements in region m.

3.2. Two-dimensional SMM

The stepwise steady-state heat conduction analysis based on the SMM of the two-dimensional rectangular geometry is presented by considering in turn the mentioned considerations in the previous section as follows:

1) Dividing each homogeneous region into three slides in each direction and then computing the heat conduction equations numerically using the iterative manner to approximate the temperature profiles (similar to eqs. (27) and (28)).

2) Using the initial calculations from the previous step, determining the corresponding weighting factors can be performed for each slide in x and y directions as:

$$SWF_l = \sum_{l;p=1}^{3} T^{l,p}, \quad p = 1,\ 2 \text{ and } 3 \tag{33}$$

$$SWF_p = \sum_{p;l=1}^{3} T^{l,p}, \quad l = 1,\ 2 \text{ and } 3 \tag{34}$$

where l and p are the total number of slides in x and y directions, respectively. Note also that CWF_l and RWF_p in eqs. (33)

and (34) refer to the slide Weighting Factor of column *l*, and row *p*, respectively. In the case of the 2-D multi-region geometries, eqs. (33) and (34) can be rewritten as:

$$SWF_{m,l} = \sum_{l;p=1}^{3} T^{m,l,p}, \qquad p = 1,\ 2 \text{ and } 3 \tag{35}$$

$$SWF_{m,p} = \sum_{p;l=1}^{3} T^{m,l,p}, \qquad l = 1,\ 2 \text{ and } 3 \tag{36}$$

Here $T^{m,l,p}$ is temperature in row *p* and column *l* in region *m*. Additionally, $CWF_{m,l}$ and $RWF_{m,p}$ in eqs. (35) and (36) refer to, respectively, the Slide Weighting Factor of column *l* and row *p* in region *m*.

3) Assigning the appropriate mesh point numbers for each column and row, according to the obtained weighting factors as below:

$$\frac{SWF_l}{\sum_l SWF_l} \times R = n_l, \tag{37}$$

$$\frac{SWF_p}{\sum_p SWF_p} \times Z = n_p, \tag{38}$$

where n_l and n_p indicate the mesh point numbers in the corresponding column *l* and row *p*, respectively. Additionally, in the above equations, *R* refers to the total number of mesh elements in *x* direction and *Z* similarly is the total number of mesh elements in *y* direction. It should be also stressed that in the case of two-dimensional, multi-regions, similar to the one-dimensional approach each homogeneous region should be treated separately via dividing each existing region into three slides in both *x* and *y* direction. In the case of 2-D multi-region geometries, one can rewrite eqs. (37) and (38) as the following:

$$\frac{SWF_{m,l}}{\sum_l SWF_{ml}} \times R_m = n_{m,l}, \tag{39}$$

$$\frac{SWF_{m,p}}{\sum_p SWF_{m,p}} \times Z_m = n_{m,p}, \tag{40}$$

where R_m and Z_m refer to the total number of mesh elements in region *m* in *x* and *y* direction, respectively. Moreover, $n_{m,l}$ and $n_{m,p}$ indicate the mesh point numbers in region *m* and in column *l* and row *p*, respectively.

4. Numerical Results

In this section, some test cases are solved numerically by the iterative process based on the SMM and the Conventional Method (CM) which employ uniform mesh distribution. The obtained results, including the maximum temperature, the location of the maximum temperature and in addition the total CPU execution time have been demonstrated to evaluate the accuracy and efficiency of the proposed method. It should be also noted that, for a consistent accuracy comparison, the results determined by the two methods have been benchmarked against the reference (exact) solutions which obtained using the grid size of 100 and 100×100 mesh elements per region for one and two-dimensional geometries, respectively.

Similar to the previous sections, this section is also divided into two main sub-sections for one and two-dimensional geometries. Where, the results for a number of study cases have been provided in each sub-section.

4.1. One-dimensional results

In the following, some numerical problems are solved to consider and compare the results of the CM and the adaptive one against the accurate solutions. The first case relates to a homogeneous region with the volumetric thermal source strength (q''') of 900 (W/m^3) and the heat conduction coefficient of 13 (W/m.K). The boundary conditions for this case study comprise of constant temperatures at the external boundaries which is presented in Fig.4.

The exact solution has a sharp peak at 0.79 (m) with the maximum temperature of 321.543 (K). Fig.5 displays the calculated temperature distributions of the CM (based on uniform distribution) and the improved one.

According to this figure, using the proposed three-step algorithm mentioned in section 3.1, a finer mesh grid is assigned to the sub-regions with corresponding higher temperature, stand in total contrast to CM. It is interesting to note that to evaluate the accuracy of the obtained results, the Relative Percent Error (*RPE*) and the Apparent Absolute Error (*AAE*) can be defined as the following equations:

$$RPE\,(\%) = \left| \frac{\text{calculated value-reference value}}{\text{reference value}} \right| \times 100, \tag{41}$$

$$AAE = \left| \text{calculated value-reference value} \right|. \tag{42}$$

The *RPE* and *AAE* results analysis for both the aforementioned methods has been given in Table 1 for 10 mesh box numbers.

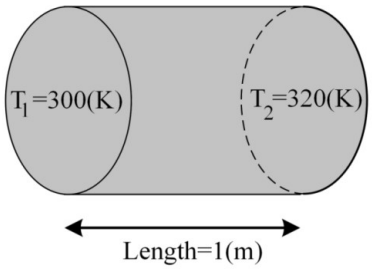

Fig. 4. Geometry of test case 1

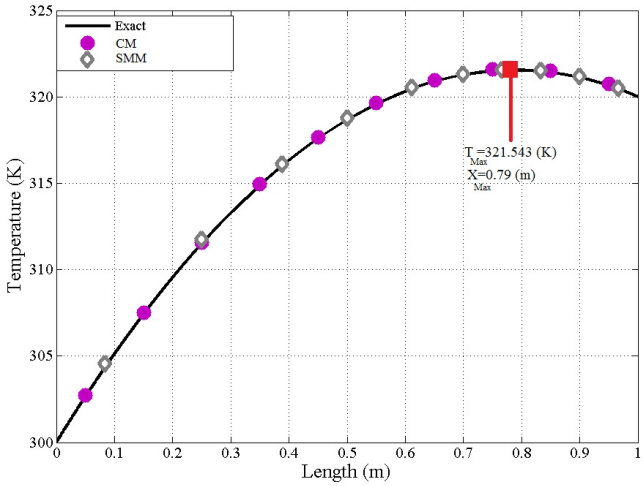

Fig. 5. Solution of the heat conduction equation based on the CM and proposed SMM for the test case 1

Table 1. *RPEs* of the calculated maximum temperatures, *AAEs* of the calculated location of maximum temperature and the total CPU execution time for the test case 1

Distribution	Number of boxes	*RPE* (%) of maximum temperature	*AAE* in location of the maximum temperature (m)	Total CPU time (s)
CM	10	0.011	0.039	0.06
SMM	10	0.007	0.022	0.06

As is evident, the obtained results by the proposed method with 0.022 (cm) is more accurate than that of the ordinary method with 0.039 (cm); on account of the fact that by optimizing the mesh point positions with respect to the trend of temperature profile, the locations of extreme values can more accurately be obtained.

The second case study is related to a one-dimensional geometry with two different regions. Fig. 6 represents the geometry and the boundary conditions of this problem.

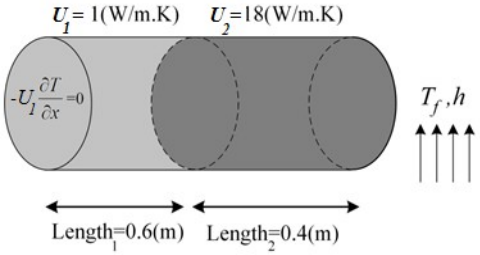

Fig. 6. Geometry of test case 2

where, q''' for the region 1 is 300 and for the region 2 is 5 (W/m^3). Additionally, the heat transfer coefficient and the flow temperature have been considered to be 2000 (W/m^2.K) and 311 (K), respectively. The exact solution has a peak at the origin

of the region 1 with the maximum temperature of 369.093 (K) and a peak at 0.60 (m) with a maximum temperature of 315.368 (K) in the region 2. Similar to the previous case study, the proposed adaptive method and the CM (based on uniform distribution) have been applied to this problem to predict the desired considerations by performing the governed equations numerically. Here, the drawn mesh point distributions based on the mentioned methods are illustrated in Fig. 7. It has been also noted that, the accuracy and efficiency of the obtained results are given in Table 2.

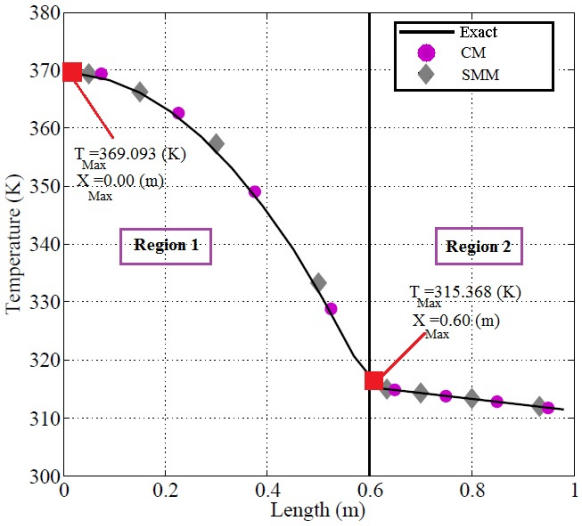

Fig.7. Solution of the heat conduction equation based on the CM and proposed SMM for the test case 2

Table 2. *RPEs* of the calculated maximum temperatures, *AAEs* of the calculated location of maximum temperature and the total CPU execution time for the test case 2

Region number	Distribution	Number of boxes	*RPE* (%) of maximum temperature	*AAE* in location of the maximum temperature (m)	Total CPU time (s)	
					CM	SMM
Region 1	CM	4	0.005	0.075	0.034	0.036
	SMM	4	0.002	0.050		
Region 2	CM	4	0.151	0.050		
	SMM	4	0.098	0.030		

As can apparently be seen, in the first region, the *RPE* results based on the proposed and ordinary method were 0.002 and 0.005, and in the second region, were 0.098 and 0.151, respectively. Moreover, as can be detected, the locations of the extreme values based on the mentioned methods have been compared to each other. Regarding the table in the first region the *AAE* of the proposed method was 0.050 m, while for the ordinary method it was 0.075 m. Also, the *AAEs* were 0.030 m and 0.050 m for the proposed and ordinary method in the second region, respectively.

The above-mentioned procedure is repeated for the test case 3, where the features of this case study are depicted in Fig.8.

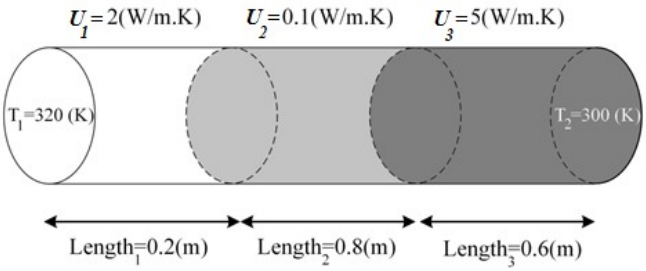

Fig. 8. Geometry of test case 3

As can be seen, this case study is comprised of three different regions with the volumetric thermal source strength of 60, 80 and 40 (W/m^3) for the region 1, 2 and 3, respectively. The accurate solution has a peak at 0.20 (m) with the maximum temperature of 324.147 (K) in the region 1, a peak at 0.57 (m) with a maximum temperature of 378.865 (K) in the region 2, and, a peak at 1.00 (m) with a maximum temperature of 306.210 (K) in the region 3. It is worth to mention that the uniform and non-uniform mesh grid structures along with the corresponding temperature distributions have been displayed in Fig. 9. Having looked at the results tabulated in Table 3, the advantages of the novel mentioned algorithm in the case of determination of the maximum values and the corresponding locations are proven.

4.2 Two-dimensional results

This section comprises of two case studies for the two-dimensional heat conduction calculations. First, we present the results of a simple homogeneous region, which is shown in Fig. 10. The length of this problem both in x and y direction is 1

(m) and the heat conduction coefficient is 4 (W/m.K). Additionally, the volumetric thermal source strength is 100 (W/m^3). The boundary conditions of this problem have been illustrated in Fig. 10. The accurate solution has the maximum temperature of 420 (K) that is located on the right side of the geometry (see Fig. 11).

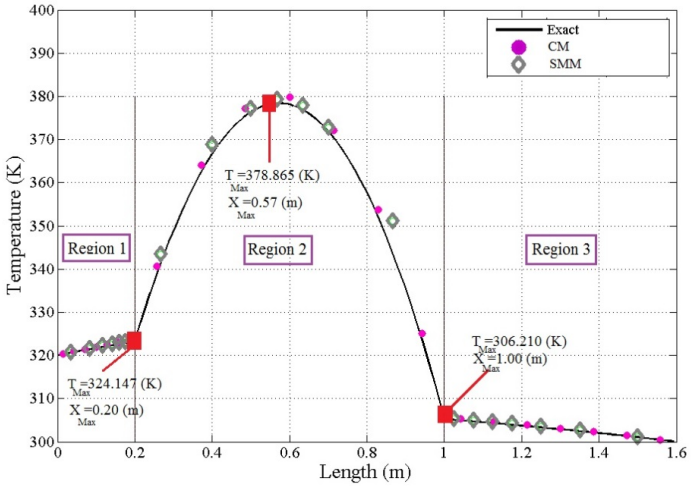

Fig. 9. Solution of the heat conduction equation based on the CM and proposed SMM for the test case 3

Table 3. *RPEs* of the calculated maximum temperatures, *AAEs* of the calculated location of maximum temperature and the total CPU execution time for the test case 3

Region number	Distribution	Number of boxes	*RPE* (%) of maximum temperature	*AAE* in location of the maximum temperature (m)	Total CPU time (s)	
					CM	SMM
Region 1	CM	7	0.014	0.056	0.051	0.056
	SMM	7	0.008	0.029		
Region 2	CM	7	0.028	0.265		
	SMM	7	0.015	0.118		
Region 3	CM	7	0.043	0.084		
	SMM	7	0.025	0.044		

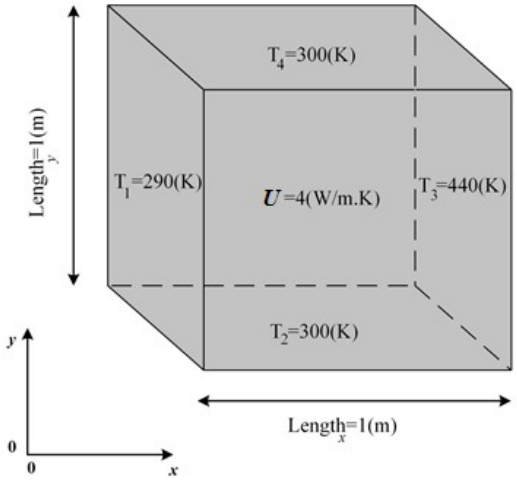

Fig. 10. Geometry of test case 4

For facilitating comparison between the mentioned methods, the results of the numerical calculations, including the errors of the obtained maximum temperatures and the corresponding locations are given in Table 4.

Table 4. *RPEs* of the calculated maximum temperatures, *AAEs* of the calculated location of maximum temperature and the total CPU execution time for the test case 4

Distribution	Number of boxes	*RPE* (%) of maximum temperature	AAE_x in location of the maximum temperature (m)	AAE_y in location of the maximum temperature (m)	Total CPU time (s)	
					CM	SMM
CM	8×8	0.017	0.049	0.042	0.081	0.085
SMM	8×8	0.009	0.025	0.026		

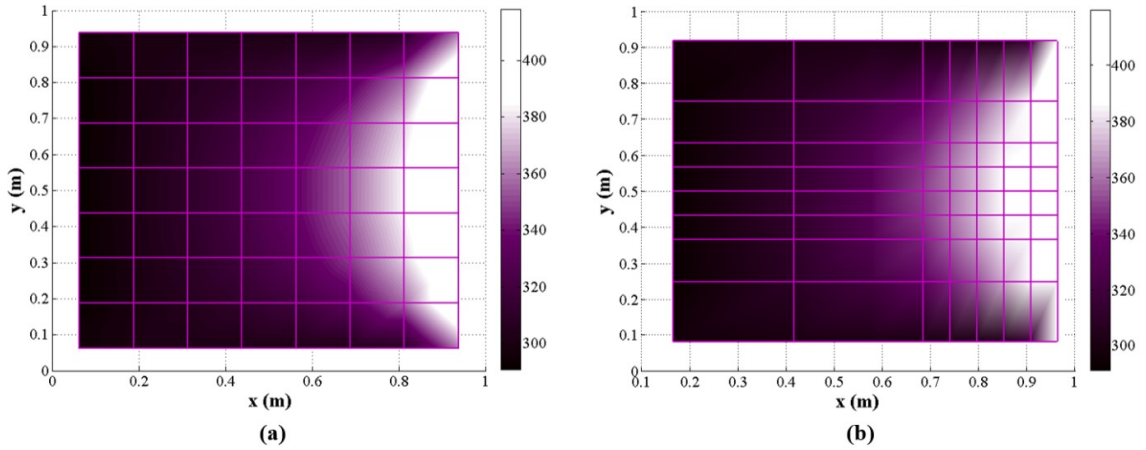

Fig. 11. Solution of the heat conduction equation based on the a) CM and b) proposed SMM for the test case 4 for grid size 8×8

As it is observed, the locations of the extreme values which are obtained based on the aforementioned methods have been compared to each other for both x and y directions. This is due to the fact that by optimizing mesh point positions in 2-D geometries, the locations of extreme values will then be optimized in two directions, consequently.

The geometry and boundary conditions of the second problem (test case 5) are shown in Fig. 12; where the volumetric thermal source strength of region 1 and 2 are 400 and 100 (W/m^3), respectively.

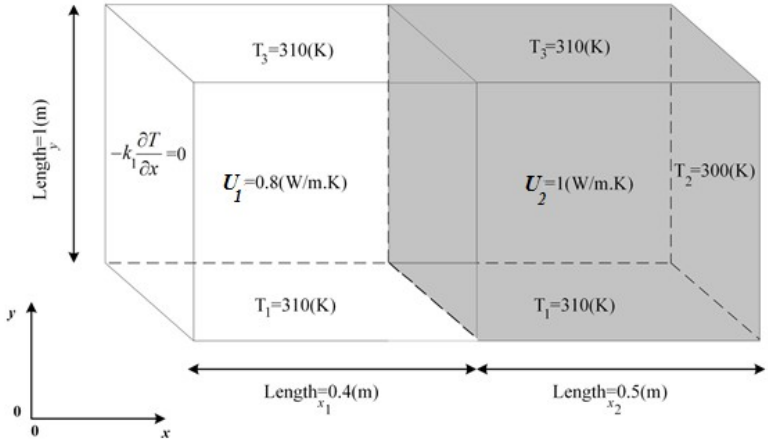

Fig. 12. Geometry of test case 5

The accurate solution has a peak at (0.00, 0.50) meter in the region 1 with the maximum temperature of 351.852 (K), and, a peak at (0.40, 0.50) meter with a maximum temperature of 334.851 (K) in the region 2. The obtained 2-D temperature distributions for uniform and non-uniform grid size 14×14 are depicted in Fig. 13.

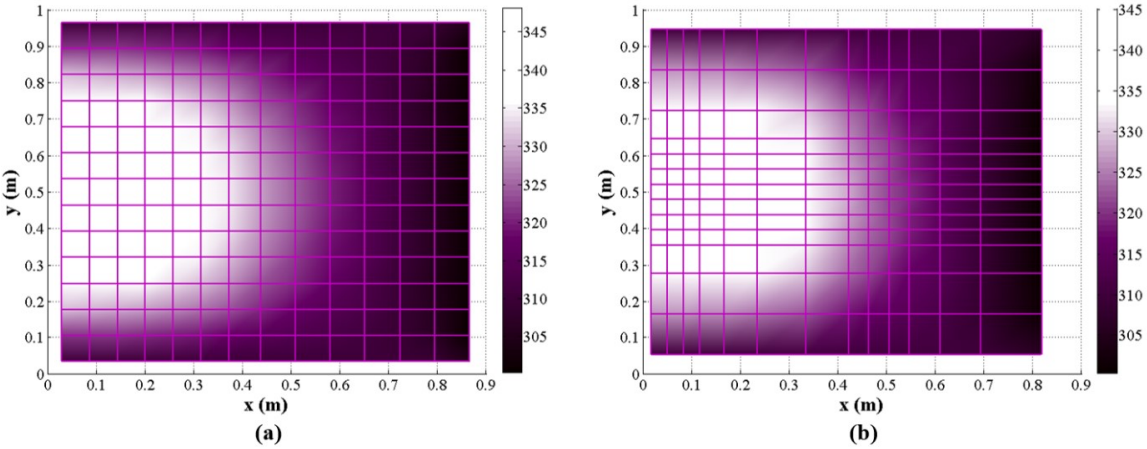

Fig. 13. Solution of the heat conduction equation based on the a) CM and b) proposed SMM for the test case 5 for grid size 14×14

In Table 5, the calculated results for both region 1 and 2 using the developed method and the CM (based on uniform distribution) are compared with the accurate solution.

Table 5. *RPEs* of the calculated maximum temperatures, *AAEs* of the calculated location of maximum temperature and the total CPU execution time of the test case 5 for grid size 14×14

Region number	Distribution	Number of boxes	*RPE* (%) of maximum temperature	AAE_x in location of the maximum temperature (m)	AAE_y in location of the maximum temperature (m)	Total CPU time (s)	
						CM	SMM
Region 1	CM	7×7	0.021	0.090	0.088	0.901	0.912
	SMM	7×7	0.015	0.057	0.059		
Region 2	CM	7×7	0.034	0.089	0.095		
	SMM	7×7	0.019	0.069	0.070		

Furthermore, in order to check the capability and accuracy of this algorithm for any arbitrary number of mesh element boxes, the proposed SMM method has been applied to a different mesh element grid size of the last case study. Fig. 14 displays the temperature distribution for uniform and non-uniform grid structure of the grid size 22×22.

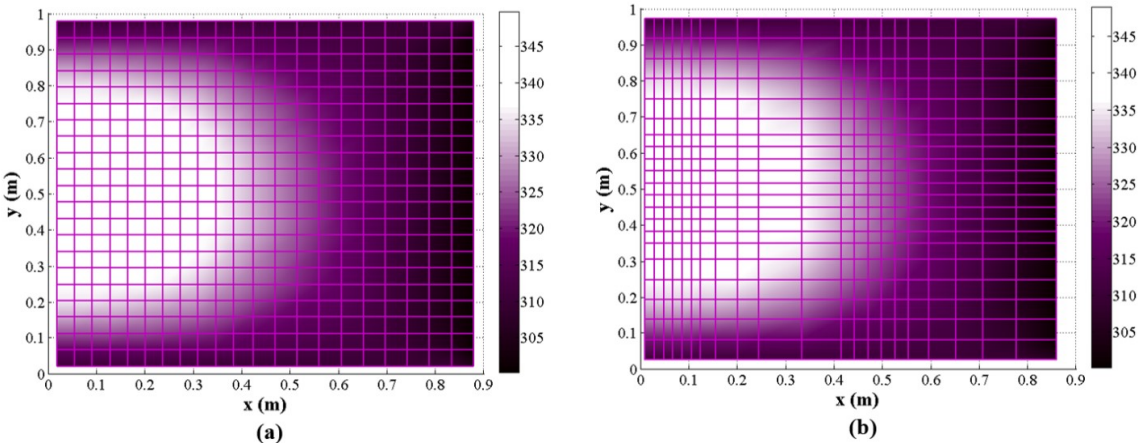

Fig. 14. Solution of the heat conduction equation based on the a) CM and b) proposed SMM for the test case 5 for grid size 22×22

The obtained results, including the *RPEs* of the maximum temperatures, *AAEs* of the location of maximum temperatures and the total CPU execution times have been tabulated for both the aforementioned distributions in the Table 6.

Table 6. *RPEs* of the calculated maximum temperatures, *AAEs* of the calculated location of maximum temperature and the total CPU execution time of the test case 5 for grid size 22×22

Region number	Distribution	Number of boxes	*RPE* (%) of maximum temperature	AAE_x in location of the maximum temperature (m)	AAE_y in location of the maximum temperature (m)	Total CPU time (s)	
						CM	SMM
Region 1	CM	11×11	0.009	0.078	0.093	1.701	1.740
	SMM	11×11	0.006	0.060	0.070		
Region 2	CM	11×11	0.011	0.090	0.100		
	SMM	11×11	0.008	0.059	0.082		

As is observed from this table, the calculated parameters have been given to the region 1 and 2, separately.

5. Discussion

As can be observed from Table 1, the *RPE* of the calculated maximum temperature based on the CM is 0.011 %, though; the obtained value of the SMM is 0.07 %. Furthermore, as is apparent the *AAEs* of the location of maximum temperature are 0.039 and 0.022 using the CM and the SMM, respectively. Similarly, it can be seen from the Tables 2, 3, 4, 5 and 6, that the suggested method gives more accurate results in comparison to the CM. However, it should be underlined that for a consistent comparison between the efficiency of the CM and the SMM, the total CPU execution time has been considered using a laptop computer with CPU 1.60 GHz.

The results (*RPEs*) in the tables indicate that the new method with non-uniform grid is indeed more accurate than the CM based on the uniform grids at a very comparable computational expense. All results presented in the paper are namely already calculated with the excellent accuracy in the order of *RPE*(%)<0.15% regardless of the method used. However, all the results indicated that about 50% improvement can be achieved by considering the proposed method without any significant extra computational CPU time. From a practical point of view, this improvement can be very useful in many technological and scientific engineering applications. For example, in nuclear safety analysis, there are some safety criteria for maintaining the maximum fuel and clad temperatures within certain limitations [21]. Accordingly, calculating and obtaining the mentioned extremes as accurate as possible without significant computational costs is vital. Additionally from a numerical point of view, it is worth bearing in mind that, for areas of interest where gradients vary significantly in space, using a fine grid over the domain can be computationally intensive. So it can be reasonably argued that using small mesh spacing where the function is varying large can be very useful. In this paper, we proposed an enhanced algorithm instead of applying complex mathematical

prospective to predict the extreme values and their corresponding locations in a number of different problems.

Based on the arguments mentioned above, it can be concluded that the proposed method has about 50% more accuracy than that of the ordinary method. Moreover, it should be noted that the total execution time of the proposed method is nearly equal to the other one. This is due to the fact that the computational cost of the primary calculations based on the SMM is not comparable with the iterative process. Consequently, one can argue that the adaptive proposed SMM is more efficient compared with CM.

From another point of view, the information about how much one has to condense the uniform grid (and concurrently increasing the computational expense) in order to obtain a similar accuracy of the results should be considered. Table 7 shows the number of additional boxes in CM, the corresponding computational cost for all of the presented benchmark problems.

Table 7. Comparison results between the CM and SMM for obtaining the same accuracy

Test Case Number	Methods	Number of boxes	*RRE* (%) of maximum temperature			in location of the maximum temperature (m)						Total CPU time (s)
			Region Number			Region Number						
						1		2		3		
			1	2	3	AAE_x	AAE_y	AAE_x	AAE_y	AAE_x	AAE_y	
1	CM	14	~0.007	…	…	~0.022	…	…	…	…	…	0.11
	SMM	10	0.007	…	…	0.022	…	…	…	…	…	0.06
2	CM	12	~0.002	~0.098	…	~0.050	…	~0.030	…	…	…	0.077
	SMM	8	0.002	0.098	…	0.050	…	0.030	…	…	…	0.036
3	CM	33	~0.008	~0.015	~0.025	~0.029	…	~0.118	…	~0.044	…	0.118
	SMM	21	0.008	0.015	0.025	0.029	…	0.118	…	0.044	…	0.056
4	CM	102	~0.009	…	…	~0.025	~0.026	…	…	…	…	0.193
	SMM	64	0.009	…	…	0.025	0.026	…	…	…	…	0.085
5	CM	332	~0.015	~0.019	…	~0.057	~0.059	~0.069	~0.070	…	…	1.907
	SMM	196	0.015	0.019	…	0.057	0.059	0.069	0.070	…	…	0.912
5	CM	820	~0.006	~0.008	…	~0.060	~0.070	~0.059	~0.082	…	…	3.801
	SMM	484	0.006	0.008	…	0.060	0.070	0.059	0.082	…	…	1.740

As is observable, more boxes and accordingly much more computational costs are needed if almost the same results are desired. This shows that the proposed SMM can improve the accuracy of the solutions in a reasonable running time.

Another important point that is worth to mention is that the proposed method is based on a simple discretization and efficient implementation. The benchmarks which were considered in this work have analytical solution [22]. However, the analytical solution relies on a relatively sophisticated mathematical solution and accordingly for practical applications, the computational cost, the complexity of implementation and sophisticated mathematical calculations associated with the analytical calculation could be overwhelming. In the following, the analytical solution of 2 dimensional heat conduction equation for a homogeneous material composition considering the constant temperature on the geometry boundaries is presented as:

$$T(x,y)=\sum_{n=1}^{\infty}\left\{\frac{2}{a\sinh\left(\frac{n\pi b}{a}\right)}\int_0^a C\sin\left(\frac{n\pi}{a}x\right)dx\right\}\sin\left(\frac{n\pi}{a}x\right)\sinh\left(\frac{n\pi}{a}y\right), \tag{43}$$

where a, b and C are, respectively, the dimension of the geometry in x and y direction and the temperature on the boundary of geometry in line b. Additionally, it should be noted that the temperature on other boundaries are considered to be zero. As is observable, the mathematical solution is sophisticated even for a simple homogeneous problem. On this basis, development of efficient solver codes for practical heat transfer applications is highly recommended.

6. Conclusion

The present work deals with an enhanced adaptive spatial mesh refinement approach for the heat conduction calculations using the SMM. This proposed method works based on dividing each homogeneous region into separate slides and then assigning different mesh point densities to slides of interest regarding their relative importance using some formulated weighting factors. These weighting factors comprise of terms which needs the approximated temperature profile in each region and slide. The proposed SMM, which allows for accurate and efficient solution of the heat conduction equation, is applied to some case studies with different geometries and boundary conditions. The numerical results showed high accuracy and efficiency of the proposed SMM compared to the Conventional Method (CM). It is also worthwhile to mention that the extra execution time for the primary required mathematical calculations was almost negligible in comparison with the total CPU time. Moreover, different grid sizes were used to consider the accuracy of the suggested method for any arbitrary mesh point numbers. Results of comparison between the SMM and the CM, proved the strength of the proposed SMM. According to the satisfactory results reported herein, it is very promising for future application of the proposed method to simulate a variety more challenging problems for which a pre-determined mesh position strategy can be established.

Conflict of Interest

The author(s) declared no potential conflicts of interest with respect to the research, authorship and publication of this article.

Funding

The author(s) received no financial support for the research, authorship and publication of this article.

Nomenclature

BSFDM	Box-Scheme Finite Difference Method	p	Number of slides in y direction for 2-D geometry
U	Heat conduction coefficient	P	Total No. of slides in y direction for 2-D geometry
T^i	Temperature of mesh box i	q'''	Volumetric thermal source strength
T^j	Temperature of mesh box j	W	Total No. of mesh elements in 1-D
T^g	Average temp. of each slides (1D geometry)	R	Total No. of mesh elements in x direction for 2-D
Δ^i	Side length of mesh box i	Z	Total number of mesh elements in y direction for 2-D
Δ^j	Side length of mesh box j	n_l	Mesh point numbers for slide l
S^i	Area of mesh box i	n_p	Mesh point numbers for slide p
V^i	Volume of mesh box i	SWF_g	Slide Weighting Factor g
g	Number of slides in 1-D	SWF_l	Slide Weighting Factor for slide l
l	Number of slides in x direction for 2-D geometry	SWF_p	Column Weighting Factor for slide p
d_g	Mesh point numbers in the corresponding slide g	σ	Stefan-Boltzmann constant
α	Radiation absorptivity		

References

[1] Bergman, Th., Lavine, A. S., Incropera, F. P., Dewitt, D. P., *Fundamentals of heat and mass transfer*. The United States, John Wiley & Sons (2011)
[2] Wakil, M. M. El., *Nuclear heat transport*. The United States, The Haddon Craftsmen Inc (1971)
[3] Wang, C., Dong, X., Shu, C. H., Parallel adaptive mesh refinement method based on WENO finite difference scheme for the simulation of multi-dimensional detonation. *J Comput Phys* 298 (2015) 161–175
[4] Fengzhi, L., Penghao, R., A novel solution for heat conduction problems by extending scaled boundary finite element method. *Int J Heat Mass Transf* 95 (2016) 678-688
[5] Wang, P., Yu, B., Li, J., Zhao, Y., Shao, Q., A novel finite volume method for cylindrical heat conduction problems. *Int Commun Heat Mass* 63 (2015) 8–16
[6] Haddad, H., Guessasma, M., Fortin, J., Heat transfer by conduction using DEM–FEM coupling method. *Comp Mater Sci* 81 (2014) 339-347
[7] Yao, W., Yu, B., Gao, X., Gao, Q., A precise integration boundary element method for solving transient heat conduction problems. *Int J Heat Mass Transf* 78 (2014) 883-891
[8] Kovtanyuk, A. E., Botkin, N. D., Hoffmann, K., Numerical simulations of a coupled radiative–conductive heat transfer model using a modified Monte Carlo method. *Int J Heat Mass Transf* 55 (2012) 649-654
[9] Zhang, X., Xiang, H., A fast meshless method based on proper orthogonal decomposition for the transient heat conduction problems. *Int J Heat Mass Transf* 84 (2015) 729-739
[10] Malmir, H., Moghaddam, N. M., Zahedinejad, E., Comparison between triangular and hexagonal modeling of a hexagonal-structured reactor core using box method. *Ann Nucl Energy* 38 (2011) 371-378
[11] Vagheian, M., Ochbelagh, D. R., Gharib, M., On an improved box-scheme finite difference method based on the relative event probabilities. *Prog Nucl Energy* 88 (2016) 33-42
[12] Cao, J., Zhoua, G., Wang, C., Dong, X., A hybrid adaptive finite difference method powered by a posteriori error estimation technique. *J Comput Appl Math* 259 (2014) 117–128
[13] Lee, T. E., Baines, M. J., Langdona, S., A finite difference moving mesh method based on conservation for moving boundary problems. *J Comput Appl Math* 288 (2015) 1–17
[14] Zhai, S. H., Weng, Z. H., Feng, X., An adaptive local grid refinement method for 2D diffusion equation with variable coefficients based on block-centered finite differences. *Appl Math Comput* 268 (2015) 284–294
[15] Zhai, S. H., Qian, I., Gui, D., Fengd, X., A block-centered characteristic finite difference method for convection-dominated diffusion equation. *Int Commun Heat Mass* 61 (2015) 1–7
[16] Mallik, R. K., Mahapatra, S. K., Sarkar, A., Neural-finite difference method (NFDM) in development of improved differential approximation (IDA) and its application for coupled conduction and radiation heat transfer in a square enclosure: An experimental validation. *Int J Heat Mass* 52 (2009) 504–515
[17] Grzywiński, M., Sluzalec, A., Stochastic convective heat transfer equations in finite differences method. *Int J Heat Mass*

Transf 43 (2000) 4003-4008.
[18] Kalis, H., Efficient finite-difference scheme for solving some heat transfer problems with convection in multilayer media. *Int J Heat Mass Transf* 43 (2000) 4467-4474
[19] Talebi, S., Kazeminejad, H. A mathematical approach to predict dry-out in a rod bundle. *Nucl Eng Des* 249 (2012) 348–356
[20] Talebi, S., Kazeminejad, H., Davilu, H., Prediction of dry-out and post dry-out wall temperature using film thickness model. *Predict Eng Des* 244 (2012) 73–82
[21] IAEA-Safety Reports Series No. 30. Accident Analysis for Nuclear Power Plants with Pressurized Water Reactors. Austria: International Atomic Energy Agency (2004)
[22] Ordonez, Miranda J., Lemonnier, D., Ezzahri Y., Joulain K., Analytical description of the radiative-conductive heat transfer in a gray medium contained between two diffuse parallel plates. *Appl Math Model* 56 (2018) 51-64.